THERMAL DEBINDING MECHANISM OF METAL INJECTION MOLDING COMPACTS IN VACUUM①

Liu Shaojun, Huang Baiyun, Qu Xuanhui, Zhong Xiaoxian, Yan Wuhua and Li Yiming
The State Key Laboratory for Powder Metallurgy,
Central South University of Technology, Changsha 410083, P. R. China

ABSTRACT The processing of the thermal debinding in vacuum using water atomized 316L stainless steel powder and wax-based multicomponent binder were systemically studied. The thermal debinding velocity in vacuum was analyzed under the conditions of different binders and different rising temperature rates, especially the low temperature thermal debinding kinetics in vacuum. The processing of thermal debinding in the flowing H_2 was also compared with the processing in vacuum. The binder removal rate in vacuum was faster than that in the flowing H_2, but the control of defect is more difficult. The reason was that the gas pressure in the green parts was higher than that in environment.

Key words powder injection molding vacuum thermal debinding

1 INTRODUCTION

During the past few years, powder injection molding (PIM) had emerged as an advanced manufacturing technology[1]. The combination of these technologies allows complex shapes to be produced to near full density and with a homogeneous microstructure for high performance application. The various processing steps of PIM had been extensively studied and were well documented in the literature[2-7], the most important factor that influenced the processing and the ultimate quality was the thermal debinding and solvent debinding, and so on. The thermal debinding mechanism had been widely understood and studied, but most of the mechanisms and kinetics researches focused on thermal debinding processing under protective atmosphere and thermal debinding in vacuum was rarely studied. In fact, for some high active and easy oxidized powder such as stainless steel and magnetometric material powder, thermal debinding in vacuum was the sole and effective thermal debinding way. So, the processing of thermal debinding in vacuum was studied systemically. The processing of thermal debinding in the flowing H_2 was also compared with the processing in vacuum.

2 EXPERIMENTAL

Water atomized 316L stainless steel powder with a mean particle size of 24.65 μm was used as the material. Due to strong friction between particles, designed powder loading about 60% (volume fraction, %) was appropriate. The tap and the pycnometer density were 3.12 g/cm^3 and 4.82 g/cm^3, respectively. The wax-based multicomponent binder systems compose of high density polypropylene and low molecular weight components stearic acid and paraffin wax. Polypropylene and paraffin wax were often used in binders as a powder wetting agent and/or as a plasticizer in order to improve the molding properties of the feedstock. The binders were designed to two symbols A_1 and A_2 based on the different wax, polypropylene and stearic acid proportion. A_1 and A_2 corresponded to binder proportion by weight were 66∶26∶5 and 66∶26∶8, respectively.

The 316L stainless steel powder and binder were mixed at 175 ℃ in a twin cam mixer with 40% (volume fraction) of binder. Disc-shaped

① Received Jul. 7, 1998; accepted Dec. 5, 1998

samples with a diameter of 20 mm and thickness of 4 mm were produced by injection molding machine. Thermal debinding of PIM compacts was processed under flowing H_2 and in vacuum respectively using different rising temperature rate reached 180, 300, 400 and 500 ℃ and held every temperature half an hour, PIM compacts were removed. In order to get the thermogravimetric analysis under the actual condition, removed mass of respective powder-binder compacts at constant elevated temperature was measured based on the weight drop of PIM compacts before and after debinded at different holding temperature. The mass percent drop compared to green PIM parts was named mass loss %.

3 RESULTS AND ANALYSIS

3.1 TGA observations

In order to determine decomposed temperature of binder constituent in the multicomponent binder, thermogravimetric analysis was used, as shown in Fig.1. From Fig.1, we can see that the decomposed temperature of PW, HDPE and SA were 164.3, 413.5 and 160 ℃ respectively.

Fig.1 Thermogravimetric analysis curve

3.2 Debinding curve under actual condition

From Fig.2, it is clear that the difference of low molecular weight components concentration, in vacuum and at the same rising temperature rate made debinding rate different. The green parts composing of A_2 binder had a faster debindng rate than that of A_1 binder. The reason was that the SA proportion in A_2 binder had more SA than that in A_1 binder. Stearic acid in low temperature range was so easily evaporated and decomposed that a great deal of fine pores and pore channels formed. The more stearic acid, the more fine pores and pore channels formed[8,9]. In green parts of the same binder, the faster debinding rising temperature rate, the lower binder removal rate. The reason was that in the low temperature which is the low molecular weight components decompose range and polypropylene does not decompose, only the evaporated and decomposed gas of low molecular weight components was removed and the pore channels formed. The low rising temperature rate that made decomposed gas have enough time to be removed to the ambient. That is to say, it could make low molecular weight components to be removed fully and form the inter-connected pore channels in green parts. In the media and high temperature, decomposed high molecular weight component gas was removed to the ambient along the formed pore channel. When rising temperature rate was high, the evaporated and decomposed low molecular weight components gas had not enough time to remove to the ambient through the pore channels. In the high temperature stage, the low and high molecular weight components were decomposed at the same time, but there are not enough pore channels, internal pressure may develop and cracks occur in

Fig.2 Debinding curve in vacuum

the green part if the diffusion rate of the decomposed gas is slower than gas formation rate. So at the same debinding temperature, the debinding rate decreased.

From Figs.3, 4, we also see from the ambient temperature to 300 ℃ stage, the binder removal rate in vacuum was faster than that in flowing H_2 gas. In the intermediate stage from 300 ~ 400 ℃, the binder removal rate in vacuum kept constant and the removal mass in flowing H_2 increased continuously and reached slowly the removal mass in vacuum. In the final stage from 400 ~ 500 ℃, the two removal masses were almost the same.

Fig.3 Debinding curve in vacuum and flowing H_2 gas, 1 ℃/ min

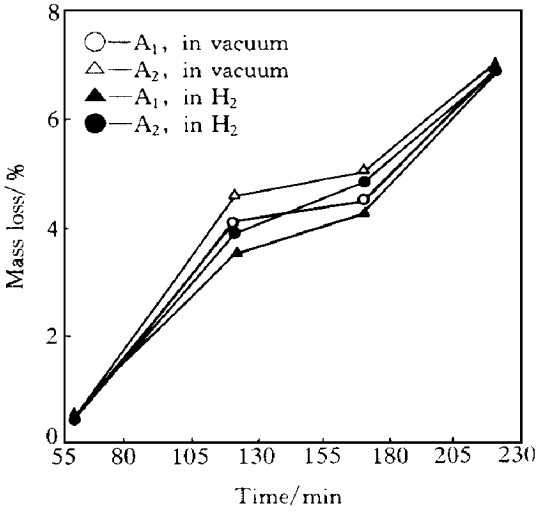

Fig.4 Debinding curve in vacuum and flowing H_2, 20 ℃/ min

4 DISCUSSION

From above experimental results, we can see that the binder removal rate was controlled by the low temperature debinding stage. In the low temperature stage, PW began to evaporate and very fine pore channels are formed through gas diffusion. In this time, the evaporation of PW was the dynamic equilibrium process between the molten PW and gasous PW. So the evaporation rate was the difference of evaporation rate and condensation rate

$$\mathrm{PW(l)} \underset{V_2}{\overset{V_1}{\rightleftharpoons}} \mathrm{PW(g)}$$

$$V_{wt} = V_1 - V_2 = K_{wt}(C_{ewt} - C_{wt}) = K_{wt}/k_g T(P_{ewt} - P_{wt})$$

where C_{ewt}(mol/cm^3) is the saturate evaporation pressure of liquid wax, C_{wt} is the evaporation concentration of environment, K_{wt} is the evaporation constant of Liquid wax, K_q is the constant of gas, T(K) is the absolute temperature. V_1(mol/s) is the evaporation rate of liquid PW; V_2 is the condensation rate, V_{wt} is the evaporation rate. So, the apparent evaporation rate of PW depends on the evaporation temperature (does not adhere to the Arrhenius, the higher temperature, the higher K_{wt}) and the pressure drop (P_{ewt}- P_{wt}). PW can evaporate only if the saturate evaporation pressure is higher than the pressure of the environment. From the analysis of microscopic aspect, at the low temperature debinding stage, the wax becomes fluid-like and is redistributed due to the caplillarity effect. In the debinding process, the molten PW will remain relatively instant, due to the action of the surface tension, the molten PW is heated and evaporated and the fine pore channels in the green part formed by the continuous evaporation of PW, and the PW in the green par decreases slowly. The contacted areas between PW and the surface of particle also decrease. The evaporation rate unit volume in the green part is denoted[10]:

$$V_{at} = A_{wt} \cdot S_{vwt} \cdot K_{wt} \cdot$$

$$X_{wt}^{awt} \cdot (P_{ewt} - P_{wt}) / K_g T$$

Where A_{wt} is the volume fraction in feedstocks; S_{vwt}(cm/cm^3) is the surface volume factor in the feedstocks; X_{wt}^{awt} is the shape factor of the surface particle in the green part. From the above equation, we can see that at the low temperature debinding stage when the vapor pressure is lower than the environmental pressure, the produced vapor is removed by atomic diffusion and transmitted to the outside of the green part. But when the vapor pressure in the green part is higher than the environmental pressure, the produced gas emitted due to the pressure drop. At this time, the vapor removed to the ambient through the forced flow and the Fick law wasn't observed. Thus, at the low temperature stage, because the pressure is always kept to zero in vacuum, the large pressure drop between the particle surface of binder and in the green parts makes evaporation rate in the surface of binder faster than that in the flowing H_2. The large pressure drop makes the vapor emit to the ambient far faster. It have more chance to produce the defect in the green part compared with the debinding in flowing H_2. In fact, in this experiment, under the same condition, debinding specimens in vacuum have more defects than that in flowing H_2 and the debinding condition must be controlled more carefully in vacuum than in flowing H_2 atmosphere. With increasing temperature, the viscosity of binder decreases and becomes fluid-like and the decomposion of binder stands leading state. The contacted areas between the binder and the ambient atmosphere increase which accelerates the decomposed rate of binder. So the removal mass of the evaporation and decomposition also increases. Due to the effect of pressure drop, the binder removal mass in vacuum is more than that in the flowing H_2.

In the intermediate, from 300 ~ 400 ℃, the binder removal mas does not change apparently, but the removal mass in the flowing H_2 increases continuously and reaches the remvoal mass in vacuum. From the above analysis, due to the pressure drop and higher binder removal rate in vacuum in the low temperature stage, PW and SA have been evaporated and removed fully, but there are still part of PW and SA that don't remove and reside in the green part in the flowing H_2. Thus, in the intermediate stage, the residual PW is decomposed and removed fully. In the final stage, from 400 ℃ to 500 ℃ proportion, the HDPE is decomposed fully when the temperature reaches 500 ℃.

5 CONCLUSIONS

(1) In vacuum, the thermal definding rate composing of different stearic acid proportion was measured. It was found that the more stearic acid proportion in binder, the higher debinding rate in the low temperature stage. The fast rising temperature rate made the chance forming the debinding defects higher and degrade finally the thermal debinding rate.

(2) The binder removal rate in vacuum was faster than that in the flowing H_2, but the defect control was more difficult. The reason was that the gas pressure in the green parts was higher than that in environment.

REFERENCE

1 Li Yimin, Qu Xuanhui, Huang Baiyun and Qiu Guanghan. Trans Nonferrous Met Soc China, 1997, 7(3): 103.

2 Qiu Guanghan, Zeng Zhoushang, Li Yimin *et al*. The Chinese Journal of Nonferrous Metals, (in Chinese), 1997, 7(4): 135.

3 German R M. Powder Injection Moulding. MPIF, New Jersey: Princeton, 1990.

4 German R M. Reviews in Particulate Materials, 1993, Vol 1, 109 - 160.

5 Angenmann H H *et al*. Inter J of Power Metal, 1993, 29(3): 239.

6 German R M. Inter J of Powder Metal, 1991, 27 (2): 127.

7 Finn C W. Inter J of Powder Metal, 1991, 27(2): 127.

8 Calvert P and Cima M. J Am Ceram Soc, 1990, 73 (3): 575.

9 Angermann H H. Inter J of Powder Metal, 1993, 29 (3): 239.

10 Huang Dianbin *et al*. Acta Metallurgica Sinica, (in Chinese), 1992, 28(2): 533.

(Edited by Zhu Zhongguo)